J Chem Biol (2010) 3:157–163
DOI 10.1007/s12154-010-0041-7

SHORT COMMUNICATION

Characterisation of the PTEN inhibitor VO-OHpic

Lok Hang Mak · Ramón Vilar · Rudiger Woscholski

Received: 9 April 2010 / Accepted: 17 May 2010 / Published online: 4 June 2010

Abstract PTEN (phosphatase and tensin homologue deleted on chromosome 10) is a phosphatidylinositol triphosphate 3-phosphatase that counteracts phosphoinositide 3-kinases and has subsequently been implied as a valuable drug target for diabetes and cancer. Recently, we demonstrated that VO-OHpic is an extremely potent inhibitor of PTEN with nanomolar affinity in vitro and in vivo. Given the importance of this inhibitor for future drug design and development, its mode of action needed to be elucidated. It was discovered that inhibition of recombinant PTEN by VO-OHpic is fully reversible. Both K_m and V_{max} are affected by VO-OHpic, demonstrating a noncompetitive inhibition of PTEN. The inhibition constants K_{ic} and K_{iu} were determined to be 27±6 and 45±11 nM, respectively. Using the artificial phosphatase substrate 3-*O*-methylfluorescein phosphate (OMFP) or the physiological substrate phosphatidylinositol 3,4,5-triphosphate (PIP_3) comparable parameters were obtained suggesting that OMFP is a suitable substrate for PTEN inhibition studies and PTEN drug screening.

Keywords PTEN · VO-OHpic · OMFP · PIP3

L. H. Mak (✉) · R. Woscholski
Division of Cell and Molecular Biology,
Imperial College London,
Exhibition Road,
London SW7 2AZ, UK
e-mail: lok.mak@imperial.ac.uk

R. Vilar
Department of Chemistry, Imperial College London,
Exhibition Road,
London SW7 2AZ, UK

Introduction

PTEN (phosphatase and tensin homologue deleted on chromosome 10) is a well-known tumour suppressor [1, 2], which loss in function through mutation, deletion, or transcriptional silencing is found in a wide spectrum of advanced human cancers [3]. It belongs to the family of the CX_5R phosphatases and was initially believed to be a tyrosine phosphatase until Maehama et al. (1998) reported that PTEN exhibits a much greater affinity towards phosphoinositides than tyrosine phosphates [4]. PTEN hydrolyses the phosphate group in the 3′ position from phosphatidylinositol 3,4,5-triphosphate (PIP_3) to form phosphatidylinositol 4,5-biphosphate and, in doing so, is counteracting phosphoinositide 3-kinases (PI3K). The balance of PTEN and PI3K activities determines the cellular PIP_3 levels, which in turn is recognised by other signalling components such as Akt [5]. Increased activity of Akt as a result of increased PIP_3 levels due to loss in PTEN function has been shown to play a major role in PTEN-mediated tumourigenesis [6]. However, there are diseases that could benefit from elevated levels of PIP_3, which could be achieved by inhibiting PTEN. In particular, wound healing [7], asthma [8], neuroprotection and regeneration [9], and indeed some cancers [10] have been linked with PTEN as a drug target.

Vanadium complexes are capable to mimic a variety of insulin-like effects, which were linked to the inhibition of protein tyrosine phosphatases (PTPs) [11–13]. More recently, it became apparent that the effects of the vanadium complexes might be due to the inhibition of PTEN [14], which could be blocked with nanomolar concentrations of vanadium inhibitors in cellular and animal models [15, 16]. Among the reported inhibitors VO-OHpic, a vanadyl compound in complex to hydroxypicolinic acid was the

most potent and specific compound [17], which has subsequently been employed to probe the role of PTEN in PI3K-dependent signalling [18] as well as PTEN-induced senescence [19]. While we gained some knowledge about PTEN's role in diseases and its potential as a possible drug target, not much is known about the mode of action of the PTEN inhibitor VO-OHpic. Therefore, we analysed the mode of PTEN inhibition by VO-OHpic, employing the natural substrate PIP_3 as well as the artificial substrate 3-*O*-methylfluorescein phosphate (OMFP).

Materials and methods

Expression and purification of PTEN

PTEN expression and purification was performed according to the methods previously described with some modifications [17]. Protein expression was induced in the *Escherichia coli* strain XL-1 blue for 24 h using 1 mM isopropyl β-D-1-thiogalactopyranoside (IPTG) at 23°C. After growth, the cells were harvested and stored at −20°C. The harvested cells were resuspended in lysis buffer containing 50 mM Tris (pH 7.4), 1% Triton X-100, 10 mM benzamidine hydrochloride, 100 μg/mL soybean trypsin inhibitor, 1 mM 4-(2-aminoethyl)benzenesulfonyl fluoride hydrochloride, and 2 mM dithiothreitol (DTT). Lysozyme was added to the cell suspension at a concentration of 2 mg/mL and stirred for 1 h at 4°C. Lysis was performed by sonication, followed by centrifugation at 18,000*g* for 1 h at 4°C. The supernatant was loaded onto a glutathione sepharose column and preequilibrated with 50 mM Tris (pH 7.4), 140 mM NaCl, and 2.7 mM KCl. After loading, the column was washed twice with 50 mM Tris (pH 7.4), 140 mM NaCl, 2.7 mM KCl, and 2 mM DTT. Another two washes were performed using the same buffer with 500 mM NaCl. The glutathione S-transferase (GST)-tagged PTEN was eluted using 20 mM glutathione in 50 mM Tris (pH 7.4), 250 mM NaCl, 20% glycerol, and 2 mM DTT. PTEN integrity was confirmed using Western blotting using GST-antibody. Protein concentration was determined using Bradford assay.

PTEN assay with OMFP as substrate

OMFP cyclohexylammonium salt was dissolved in dimethyl sulfoxide (DMSO) to a concentration of 20 mM and then further diluted with 1% DMSO to the tested concentrations. Assays were performed in 100 mM Tris (pH 7.4) containing 2 mM DTT at room temperature (RT) (20°C). Reactions were initialised by adding OMFP to the PTEN buffer mixture. The hydrolysis of OMFP to OMF was monitored by measuring the change of fluorescence units in a 96-well microtiter plate (excitation at 485 nm and emission at 525 nm) using a Varian fluorescence spectrophotometer. In the course of testing OMFP as a substrate for PTEN, methanol and DMSO were used as the solvent to dissolve OMFP. Although no significant differences were found between the two solvent systems, DMSO is the preferred solvent to use as a stock solution of 20 mM can be made (with sonication), whereas OMFP could only be dissolved at a concentration of 4 mM in methanol. Therefore, by using DMSO, the final solvent concentration in the assay can be kept low, as high concentration of solvent can have an impact on enzyme activity and stability. When using OMFP at high concentration (>1 mM), inner filter effect due to absorption can decrease the measured fluorescence intensity and therefore distort the kinetic analysis. The inner filter effect can be simply verified by measuring the high substrate sample by dilution [20, 21]. If inner filter effects are present, the observed fluorescence intensities must be corrected.

PTEN assay with PIP_3 as substrate

Enzyme activity of PTEN was measured in 100 mM Tris (pH 7.4) containing 2 mM DTT. PIP_3, diC16 sodium salt, was dissolved in distilled water to a final concentration of 1 mM and then further diluted with water to the tested substrate concentration. The assay was performed at 30°C for 20 min. In order to stop the reaction 2.25 volume of colour reagent (5 mM malachite green, 17 mM ammonium heptamolybdate, 77 mM bismuth citrate and 1.7 M HCl) was added to the assay. The mixture was allowed to develop for 10 min, and the absorbance was read at 650 nm.

PTEN activity assay in the presence of 3-hydroxypicolinate vanadium (IV) (VO-OHpic) complex

K_m and V_{max} determination in the presence of VO-OHpic

$[V(=O)(H_2O)(OHpic)_2]$ (herein referred to as VO-OHpic) was prepared following a previously reported procedure [22]. VO-OHpic was dissolved in DMSO (100 μM) and diluted further to the required concentration with 1% DMSO. For inhibition studies, PTEN was preincubated with VO-OHpic at RT for 10 min before substrate was added to initialise the reaction. Background absorbance (malachite green assay) and fluorescence (OMFP assay) were determined with VO-OHpic in assay buffer and corrected in the data analysis.

Reversibility of VO-OHpic inhibition—inhibitor dilution assay

In order to study the reversibility of the VO-OHpic inhibition, PTEN was preincubated with a high concentration of inhibitor and then diluted by adding reaction buffer

with no inhibitor present. The remaining PTEN activity towards OMFP was then measured and compared to the controls. The following experiments were performed in order to study the reversibility of VO-OHpic inhibition:

Experiment 1 PTEN activity in the absence of the inhibitor. PTEN was incubated at RT for 10 min in assay buffer with 1% DMSO. Six microliters of a 5.2 mM OMFP stock solution was added (final concentration, 200 μM), and the changes in fluorescence were measured.

Experiment 2 PTEN activity in the presence of 30 nM VO-OHpic. PTEN was incubated with 30 nM VO-OHpic at RT for 10 min in assay buffer with 1% DMSO (total volume, 150 μL). Six microliters of a 5.2 mM OMFP stock solution was added (final concentration, 200 μM), and the changes in fluorescence were measured.

Experiment 3 PTEN activity in the presence of 30 nM VO-OHpic after dilution. PTEN was incubated with 300 nM VO-OHpic at RT for 10 min (15 μL). After preincubation, 135 μL of assay buffer containing 1% DMSO was added. The resulting VO-OHpic concentration was 30 nM. The mixture was allowed to incubate for 10 min at RT, and then OMFP was added (as above) and the fluorescence changes were measured.

Experiment 4 PTEN activity in the presence of 300 nM VO-OHpic after dilution. As under 3, PTEN was preincubated with 300 nM VO-OHpic (15 μL), and after 10 min, 135 μL of 300 nM VO-OHpic in assay buffer with 1% DMSO was added and incubate for 10 min at RT. Again, OMFP to a final concentration of 200 μM was added and the fluorescence monitored.

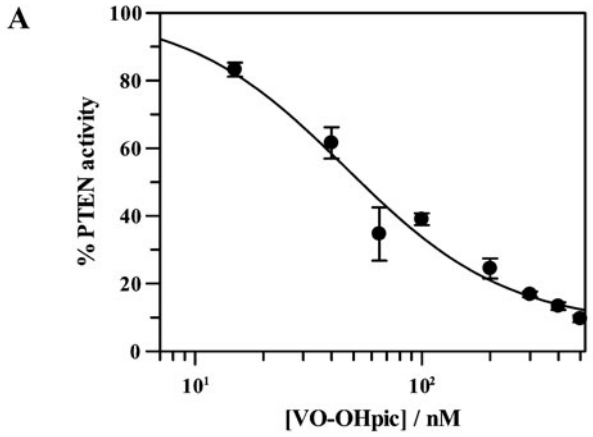

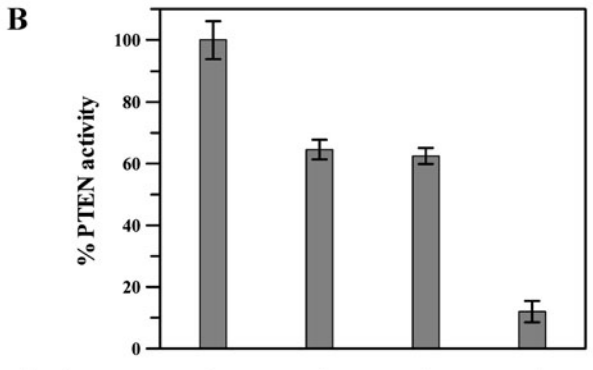

Experiment no.	1	2	3	4
Initial[VO-OHpic]	0 nM	30 nM	300 nM	300 nM
[VO-OHpic] in dilution buffer	-/-	-/-	0 nM	300 nM
Final[VO-OHpic]	0 nM	30 nM	30 nM	300 nM

Fig. 2 **a** IC_{50} determination of VO-OHpic with OMFP as substrate. PTEN was preincubated with VO-OHpic with the indicated concentrations at RT. Reactions were started by adding 200 μM of OMFP. The results are the average ± the standard deviations of three independent experiments. Data analyses were performed using GraFit. Inhibition data were fitted to a four-parameter logistic equation. **b** Reversibility of PTEN inhibition by VO-OHpic by dilution. The inhibitor dilution assays were performed as described in the Materials and methods section. Data shown are relative to the PTEN activity in the absence of VO-OHpic (experiment 1). The results are presented as the mean ± the standard deviation of three independent experiments

Results and discussion

Reversibility of VO-OHpic inhibition

Vanadium complexes have the ability to inhibit phosphatases in a reversible [23–25] or irreversible fashion [26, 27]. Prior to any further characterisation, the reversibility of the

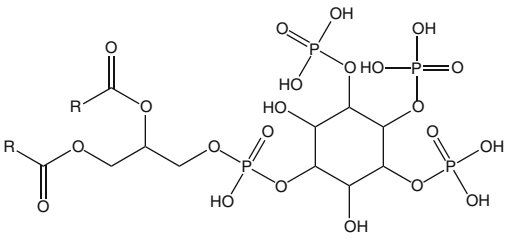

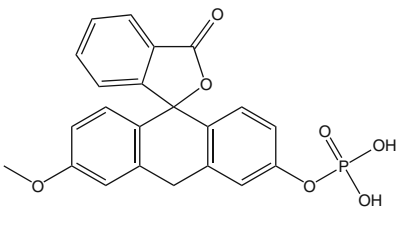

Fig. 1 Structures of PIP_3 and OMFP

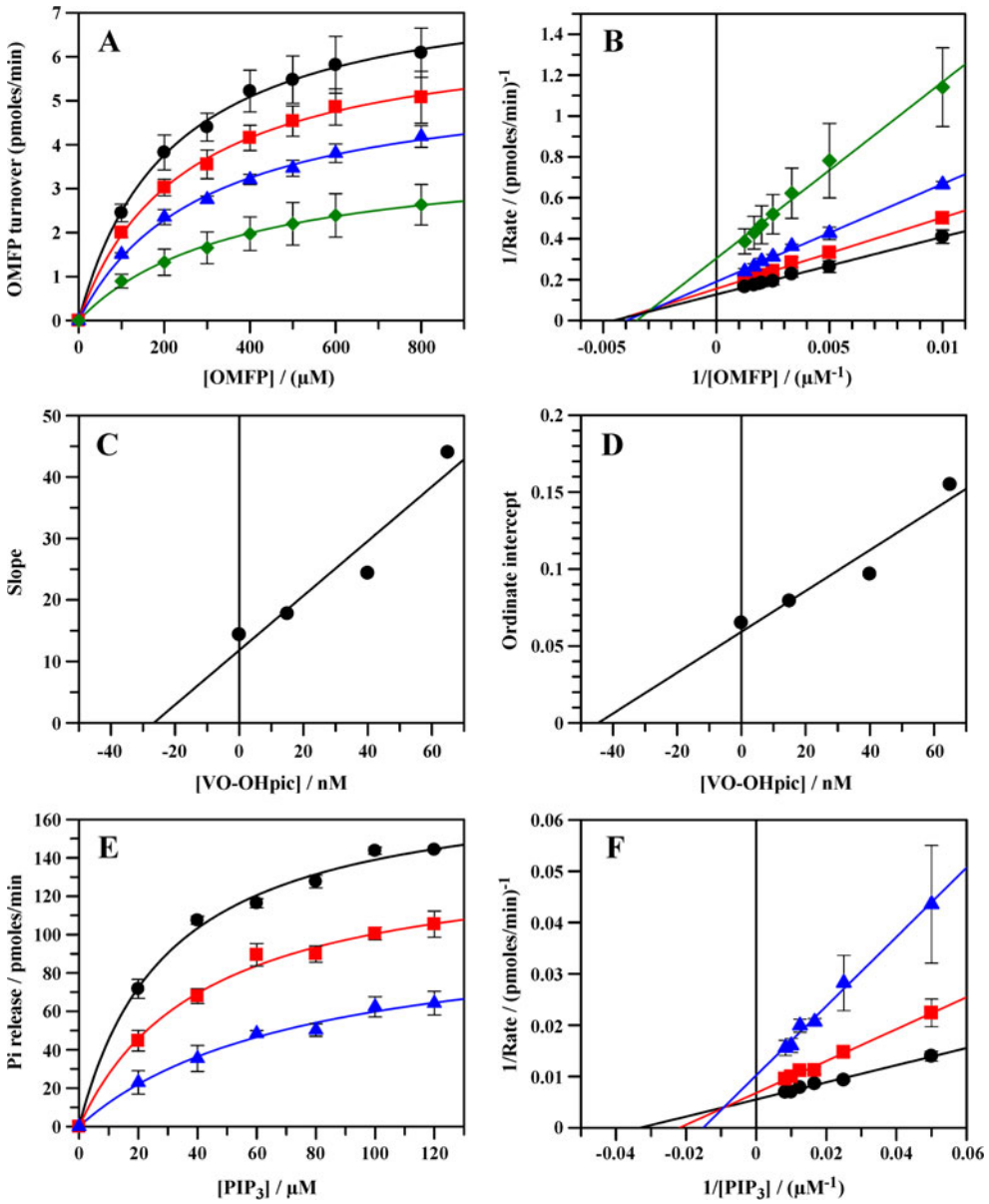

Fig. 3 **a**: Michaelis–Menten plot of PTEN activity using OMFP as substrate with increasing concentration of VO-OHpic. The VO-OHpic concentrations studied and calculated K_m and V_{max} values are as follows: 0 nM (*circles*), K_m=216±14 μM, V_{max}=7.8±0.2 pmol/min; 15 nM (*squares*) K_m^{app}=251±17 μM, V_{max}^{app}=6.7±0.2 pmol/min; 40 nM (*triangles*) K_m^{app}=291±23 μM, V_{max}^{app}=5.6±0.2 pmol/min; 65 nM (*diamonds*) K_m^{app}=375±28 μM, V_{max}^{app}=3.8±0.1 pmol/min. The results are presented as the mean ± the standard deviation of three independent experiments. **b** Lineweaver–Burk plots of kinetic data from Fig. 2a. **c** Secondary plot of the slopes of the Lineweaver–Burk plots from Fig. 2b vs. the inhibitor concentration. K_{ic} of 27±6 nM is determined as the additive inverse abscissa intercept. **d** Secondary plot of the *y*-axis intercepts from Fig. 2b vs. the inhibitor concentration. K_{iu} is determined to be 45±11 nM. **e** Michaelis–Menten plots of PTEN activity using PIP_3 as substrate with increasing concentration of VO-OHpic. The kinetics parameters calculated at the different concentration of VO-OHpic are as follows: 0 nM VO-OHpic (circles), K_m=30±4 μM, V_{max}=181±7 pmol/min; 40 nM (squares), K_m^{app}=43±6 μM, V_{max}^{app}=143±8 pmol/min; 65 nM (triangles), K_m^{app}=75±14 μM, V_{max}^{app}=104±10 pmol/min. The results are presented as the mean ± the standard deviation of three independent experiments unless otherwise stated. **f** Lineweaver–Burk plots of kinetic data from Fig. 2e. K_{ic} is determined to be 17±8 nM, and K_{iu} is determined to be 74±31 nM (n=2)

PTEN inhibitor VO-OHpic, a vanadyl complex (V^{4+}), needed to be determined. In order to achieve this, inhibitor dilution assays, which have been successfully applied to characterise catalase inhibitors [28], were employed. The artificial substrate OMFP (Fig. 1) has been used for PTPs [29–31] as well as PTEN [32] to monitor their activities, and due to its nature, it enables high throughput assays [33]. To validate the suitability of OMFP as a substrate for

testing PTEN inhibitors, we determined the potency (IC_{50} value) of VO-OHpic and subsequently compared it to the published potency of this inhibitor in a PIP_3-based assay. As shown in Fig. 2a, VO-OHpic significantly inhibits PTEN activity in low nanomolar concentrations (IC_{50}, 46± 10 nM), which is in agreement with the previously determined potency (IC_{50}, 35±2 nM) in a PIP_3-based assay [17]. Having confirmed that OMFP is a suitable substrate for PTEN activity and inhibitor measurements, recombinant PTEN was subjected to an inhibitor dilution assay with OMFP as a substrate.

If the inhibition is reversible, the PTEN activity should be recoverable upon dilution of the inhibitor concentration. In contrast, if the compound would bind irreversibly, then no significant change of activity should occur upon dilution. Thus, the PTEN phosphatase was expressed in bacteria, purified, and preincubated with or without VO-OHpic at the indicated concentration (Fig. 2b). After dilution with buffer with or without VO-OHpic being present, the remaining PTEN activity was determined with OMFP as a substrate. PTEN was preincubated with 300 nM VO-OHpic for 10 min at RT in order to achieve a strong inhibition without leaving the linearity zone. As shown in Fig. 2a, at this inhibitor concentration, the remaining PTEN activity is roughly 20% as compared to the PTEN activity without inhibitor. Upon 10-fold dilution of the initial 300 nM VO-OHpic concentration to 30 nM, the remaining PTEN activity is determined. As shown in Fig. 2b, the 10-fold dilution rescues the PTEN activity, since the remaining activity is 63% (bar 3) as compared to the noninhibited PTEN reaction (bar 1). The rescued activity upon dilution is similar to the PTEN activity that was subjected to a preincubation with 30 nM VO-OHpic, but without any dilution (bar 2). However, if the dilution was performed using a buffer containing the same concentration of VO-OHpic (300 nM), no rescue of the PTEN activity could be observed (bar 4). Taken together, these data demonstrate that the inhibition of VO-OHpic can be overcome by dilution, indicating that the PTEN inhibitor is binding to its target in a reversible fashion.

Mode of VO-OHpic inhibition

In order to investigate the mode of inhibition of VO-OHpic, the enzymological properties of PTEN towards the substrate OMFP needed to be determined. As shown in Fig. 3, both K_m and V_{max} are affected by VO-OHpic. Lineweaver–Burk plots of the same data illustrate the changes of K_m and V_{max} as the inhibitor concentration changes. In the presence of increasing amounts of VO-OHpic, the K_m shifts to higher values, whereas the V_{max} drops to lower values as can be seen in Fig. 3a. Since an increase in K_m and a decrease in V_{max} are the characteristics of a mixed type inhibition where the inhibitor can bind both the free enzyme (E) and the enzyme–substrate (ES) complex (Fig. 4), it can be concluded that VO-OHpic is a noncompetitive inhibitor with respect to OMFP as a substrate. This is in contrast to other vanadium complexes where inhibition towards PTPs is reported to be competitive with vanadium (V) [23] and vanadium (IV) [25] complexes, implying that PTEN distinguishes itself from the wider CX_5R phosphatase family not just with respect to its preferences towards inositol lipids, but also with respect to its enzymological characteristics and properties.

The data presented in Fig. 3 allowed us to determine the dissociation constants K_{ic} (EI complex) and K_{iu} (ESI complex) by plotting the slopes and y-axis intercepts from the Lineweaver–Burk plots vs. the inhibitor concentration (Fig. 3c and d, respectively). Values for K_{ic} and K_{iu} were determined as 27±6 and 45±11 nM, respectively, revealing that there is no significant difference between these parameters. Thus, one can conclude that the inhibitor binds with similar affinity to the free enzyme and the ES complex, the presence of bound substrate being without influence on the inhibitor's affinity. Given that VO-OHpic is a noncompetitive inhibitor (Fig. 3), a mode of inhibition that is normally associated with the inhibitor binding at a distinct site as compared to the substrate, it is surprising that K_{ic} and K_{iu} are very similar. VO-OHpic with two OHpic ligands and an oxo ligand is a sterically demanding molecule, and one would therefore expect that bound substrate would affect the subsequent binding of the inhibitor due to steric hindrance. However, this seems not be the case, and it is possible that the very shallow catalytic cavity of the PTEN phosphatase [34] might facilitate the accommodation of the bulky substrate and inhibitor.

For comparison, PTEN activity assays were performed with its physiological substrate PIP_3 in the absence and presence of VO-OHpic. The K_m for the uninhibited PTEN towards PIP_3 is 30 ± 4 μM, which is in good agreement with published values [35, 36]. As shown in Fig. 3e,

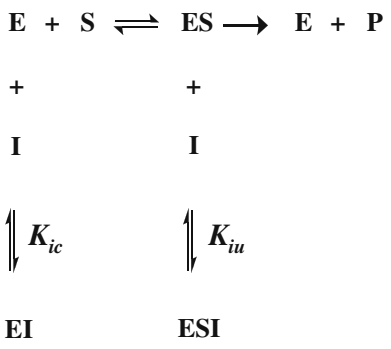

Fig. 4 Characteristic of a noncompetitive inhibition. The inhibitor (I) can bind the free enzyme (E) to form EI with the dissociation constant K_{ic} and the ES complex to form ESI with the dissociation constant K_{iu}

employing PIP_3 produced similar kinetic characteristics for the PTEN inhibitor VO-OHpic to the ones observed with the artificial substrate OMFP. With increasing concentration of VO-OHpic, an increase in K_m and a corresponding decrease in V_{max} are detected. K_{ic} and K_{iu} calculations reveal that both dissociation constants are of similar magnitude, indicating that VO-OHpic binds with similar affinity to both free enzyme E and ES complex even with PIP_3 as the substrate. Therefore, the observed PTEN inhibitor's mode of inhibition is independent of the choice of substrate.

It has been suggested that vanadium compounds are merely delivering vanadate to the catalytic site [25], since vanadyl compounds show similar potency (K_i, 0.1–0.6 μM) and mode of inhibition (competitive) as the inorganic analogue $VOSO_4$ (K_i, 0.1 μM) towards tyrosine phosphatases [37]. However, this does not seem to be the case for VO-OHpic. Firstly, VO-OHpic has a very high selectivity towards PTEN and inhibits PTPs in the high micromolar range [17]. If the compounds' mode of action was due to a delivery of the vanadyl moiety, one would expect to see similar potencies on PTPs and PTEN, since $VOSO_4$ is a nonspecific inhibitor. Secondly, the mode of inhibition for $VOSO_4$ does not match the mode of inhibition of VO-OHpic. The different binding characteristics are excluding the possibility of VO-OHpic being a vanadyl delivery tool. Therefore, it can be concluded that VO-OHpic is the active compound for the observed PTEN inhibition.

In summary, the presented data demonstrate the usefulness of OMFP for PTEN activity measurements and elucidate the mode of inhibition for VO-OHpic. The latter turned out to be of noncompetitive nature, which distinguishes the lipid phosphatase PTEN from the PTPs. This mode of inhibition is also incompatible with a vanadyl delivery role, thus, validating the vanadium-based compounds as specific phosphatase inhibitors and potential insulin-enhancing drugs.

Acknowledgments This work was supported by the Leverhulme Trust project grant (project reference, F/07 058/AO).

References

1. Li J, Yen C, Liaw D, Podsypanina K, Bose S, Wang SI, Puc J, Miliaresis C, Rodgers L, McCombie R, Bigner SH, Giovanella BC, Ittmann M, Tycko B, Hibshoosh H, Wigler MH, Parsons R (1997) PTEN, a putative protein tyrosine phosphatase gene mutated in human brain, breast, and prostate cancer. Science 275 (5308):1943–1947
2. Steck PA, Pershouse MA, Jasser SA, Yung WKA, Lin H, Ligon AH, Langford LA, Baumgard ML, Hattier T, Davis T, Frye C, Hu R, Swedlund B, Teng DHR, Tavtigian SV (1997) Identification of a candidate tumour suppressor gene, MMAC1, at chromosome 10q23.3 that is mutated in multiple advanced cancers. Nat Genet 15(4):356–362
3. Chalhoub N, Baker SJ (2009) PTEN and the PI3-kinase pathway in cancer. Annu Rev Pathol: Mech Dis 4(1):127–150
4. Maehama T, Dixon JE (1998) The tumor suppressor, PTEN/MMAC1, dephosphorylates the lipid second messenger, phosphatidylinositol 3, 4, 5-trisphosphate. J Biol Chem 273(22):13375–13378
5. Carracedo A, Pandolfi PP (2008) The PTEN-PI3K pathway: of feedbacks and cross-talks. Oncogene 27(41):5527–5541
6. Blanco-Aparicio C, Renner O, Leal JFM, Carnero A (2007) PTEN, more than the AKT pathway. Carcinogenesis 28(7):1379–1386
7. Zhao M (2007) PTEN: a promising pharmacological target to enhance epithelial wound healing. Br J Pharmacol 152(8):1141–1144
8. Lai JP, Dalton JT, Knoell DL (2007) Phosphatase and tensin homologue deleted on chromosome ten (PTEN) as a molecular target in lung epithelial wound repair. Br J Pharmacol 152 (8):1172–1184
9. Chang N, El-Hayek YH, Gomez E, Wan Q (2007) Phosphatase PTEN in neuronal injury and brain disorders. Trends Neurosci 30 (11):581–586
10. Salmena L, Carracedo A, Pandolfi PP (2008) Tenets of PTEN tumor suppression. Cell 133(3):403–414
11. Heyliger C, Tahiliani A, McNeill J (1985) Effect of vanadate on elevated blood glucose and depressed cardiac performance of diabetic rats. Science 227(4693):1474–1477
12. Rumora L, Shaver A, Zanic-Grubisic T, Maysinger D (2001) Differential regulation of JNK activation and MKP-1 expression by peroxovanadium complexes. Neurochem Int 38(4):341–347
13. Bevan AP, Burgess JW, Yale JF, Drake PG, Lachance D, Baquiran G, Shaver A, Posner BI (1996) In vivo insulin mimetic effects of pV compounds: role for tissue targeting in determining potency (vol 31, pg E60, 1995). Am J Physiol Endocrinol Metabol 33(6): U17–U
14. Schmid AC, Byrne RD, Vilar R, Woscholski R (2004) Bisperoxovanadium compounds are potent PTEN inhibitors. FEBS Lett 566(1–3):35–38
15. Rickle A, Behbahani H, Ankarcrona M, Winblad B, Cowburn RF (2006) PTEN, Akt, and GSK3beta signalling in rat primary cortical neuronal cultures following tumor necrosis factor-alpha and *trans*-4-hydroxy-2-nonenal treatments. J Neurosci Res 84 (3):596–605
16. Wang XT, Pei DS, Xu J, Guan QH, Sun YF, Liu XM, Zhang GY (2007) Opposing effects of bad phosphorylation at two distinct sites by Akt1 and JNK1/2 on ischemic brain injury. Cell Signal 19 (9):1844–1856
17. Rosivatz E, Matthews JG, McDonald NQ, Mulet X, Ho KK, Lossi N, Schmid AC, Mirabelli M, Pomeranz KM, Erneux C, Lam EWF, Vilar R, Woscholski R (2006) A small-molecule inhibitor for phosphatase and tensin homologue deleted on chromosome 10 (PTEN). ACS Chem Biol 1(12):780–790
18. Papakonstanti EA, Ridley AJ, Vanhaesebroeck B (2007) The p110 delta isoform of PI 3-kinase negatively controls RhoA and PTEN. EMBO J 26(13):3050–3061
19. Alimonti A, Nardella C, Chen Z, Clohessy JG, Carracedo A, Trotman LC, Cheng K, Varmeh S, Kozma SC, Thomas G, Rosivatz E, Woscholski R, Cognetti F, Scher HI, Pandolfi PP (2010) A novel type of cellular senescence that can be enhanced in mouse models and human tumor xenografts to suppress prostate tumorigenesis. J Clin Investig 120(3):681–693
20. Bagossi P, Kádas J, Miklóssy G, Boross P, Weber IT, Tözsér J (2004) Development of a microtiter plate fluorescent assay for inhibition studies on the HTLV-1 and HIV-1 proteinases. J Virol Meth 119(2):87–93
21. Liu Y, Kati W, Chen C-M, Tripathi R, Molla A, Kohlbrenner W (1999) Use of a fluorescence plate reader for measuring kinetic

parameters with inner filter effect correction. Anal Biochem 267 (2):331–335
22. Nakai M, Sekiguchi F, Obata M, Ohtsuki C, Adachi Y, Sakurai H, Orvig C, Rehder D, Yano S (2005) Synthesis and insulin-mimetic activities of metal complexes with 3-hydroxypyridine-2-carboxylic acid. J Inorg Biochem 99(6):1275–1282
23. Huyer G, Liu S, Kelly J, Moffat J, Payette P, Kennedy B, Tsaprailis G, Gresser MJ, Ramachandran C (1997) Mechanism of inhibition of protein–tyrosine phosphatases by vanadate and pervanadate. J Biol Chem 272(2):843–851
24. Gordon JA, Tony H, Bartholomew MS (1991) [41] Use of vanadate as protein–phosphotyrosine phosphatase inhibitor. In: Methods in enzymology: Academic Press, pp 477–82
25. Peters KG, Davis MG, Howard BW, Pokross M, Rastogi V, Diven C, Greis KD, Eby-Wilkens E, Maier M, Evdokimov A, Soper S, Genbauffe F (2003) Mechanism of insulin sensitization by BMOV (bis maltolato oxo vanadium); unliganded vanadium (VO4) as the active component. J Inorg Biochem 96 (2–3):321–330
26. Mikalsen S-O, Kaalhus O (1998) Properties of pervanadate and permolybdate. J Biol Chem 273(16):10036–10045
27. Scrivens PJ, Alaoui-Jamali MA, Giannini G, Wang T, Loignon M, Batist G, Sandor VA (2003) Cdc25A-inhibitory properties and antineoplastic activity of bisperoxovanadium analogues. Mol Cancer Ther 2(10):1053–1059
28. Margoliash E, Novogrodsky A, Schejter A (1960) Irreversible reaction of 3-amino-1:2:4-triazole and related inhibitors with the protein of catalase. Biochem J 74:339–348
29. Gottlin EB, Xu X, Epstein DM, Burke SP, Eckstein JW, Ballou DP, Dixon JE (1996) Kinetic analysis of the catalytic domain of human Cdc25B. J Biol Chem 271(44):27445–27449
30. Wang W-Q, Bembenek J, Gee KR, Yu H, Charbonneau H, Zhang Z-Y (2004) Kinetic and mechanistic studies of a cell cycle protein phosphatase Cdc14. J Biol Chem 279(29):30459–30468
31. Sun J-P, Wang W-Q, Yang H, Liu S, Liang F, Fedorov AA, Almo SC, Zhang Z-Y (2005) Structure and biochemical properties of PRL-1, a phosphatase implicated in cell growth, differentiation, and tumor invasion. Biochemistry 44(36):12009–12021
32. Li L, Ernsting BR, Wishart MJ, Lohse DL, Dixon JE (1997) A family of putative tumor suppressors is structurally and functionally conserved in humans and yeast. J Biol Chem 272(47):29403–29406
33. Johnston PA, Foster CA, Shun TY, Skoko JJ, Shinde S, Wipf P, Lazo JS (2007) Development and implementation of a 384-well homogeneous fluorescence intensity high-throughput screening assay to identify mitogen-activated protein kinase phosphatase-1 dual-specificity protein phosphatase inhibitors. Assay Drug Dev Technol 5(3):319–332
34. Lee JO, Yang HJ, Georgescu MM, Di Cristofano A, Maehama T, Shi YG, Dixon JE, Pandolfi P, Pavletich NP (1999) Crystal structure of the PTEN tumor suppressor: implications for its phosphoinositide phosphatase activity and membrane association. Cell 99(3):323–334
35. Maehama T, Taylor GS, Dixon JE (2001) PTEN and myotubularin: novel phosphoinositide phosphatases. Annu Rev Biochem 70(1):247–279
36. McConnachie G, Pass I, Walker SM, Downes CP (2003) Interfacial kinetic analysis of the tumour suppressor phosphatase, PTEN: evidence for activation by anionic phospholipids. Biochem J 371:947–955
37. Seale AP, de Jesus LA, Kim S-Y, Choi Y-H, Lim HB, Hwang C-S, Kim Y-S (2005) Development of an automated protein-tyrosine phosphatase 1B inhibition assay and the screening of putative insulin-enhancing vanadium(IV) and zinc(II) complexes. Biotechnol Lett 27(4):221–225